Diffusion and reaction in a lamellar system: Self-similarity with finite rates of reaction

F. J. Muzzio
Department of Chemical Engineering, University of Massachusetts, Amherst, Massachusetts 01003

J. M. Ottino
Department of Chemical Engineering, University of Massachusetts, Amherst, Massachusetts 01003 and Center for Turbulence Research, Stanford University, Stanford, California 94305

(Received 30 April 1990)

The evolution of an imperfectly mixed system—mimicked in terms of a distribution of lamellae—is studied. Two reactants A and B, initially placed in alternate striations, diffuse and undergo a reaction $A+B\rightarrow 2P$ with intrinsic rate $r=k_r(c_Ac_B)^\alpha$. Simulations, scaling analysis, and space-averaged (fractal) kinetics are used to study the evolution of the system for different values of α and k_r. For $\alpha=1$ and short times, a model based on the dynamics of reaction for a single lamella with infinite neighbors predicts the overall rate of reaction. For $\alpha<2.5$, diffusion takes control of the dynamics for moderate to large times, and the kinetic parameters become irrelevant. Under these conditions, critical self-organization determines the behavior of the system, and the spatial structure evolves into a self-similar form that is independent of both k_r and initial conditions. En route to scaling, the system undergoes two independent transitions: (i) from intrinsic chemical kinetics control to diffusion control, and (ii) from a system with several characteristic lengths to a system with only one characteristic length; these transitions might occur in any order, depending on controlling parameters. A combination of both short- and long-time regimes gives an efficient prediction for the average concentration of reactants for all times.

INTRODUCTION

Most of the essential aspects of mixing of miscible reacting fluids can be modeled by a one-dimensional array of striations, undergoing stretching and folding—capturing the fluid-mechanical aspects of the problem—and superposed to this fabric, diffusion and reaction.[1] This approach is the backbone of the lamellar model[2–4] which assumes that at time $t=0$, the reactants are arranged in a one-dimensional lamellar structure previously generated by the fluid mechanics (Fig. 1). After that, fluid motion stretches the striations, reducing the diffusional distances and increasing the contact area. In the most general case, both the evolution of the concentration field and the overall rate of reaction depend on mechanical mixing (stretching and folding), as well as on molecular diffusion and chemical kinetics.

In previous work,[5,6] we developed an algorithm that simulates lamellar systems undergoing an infinitely fast reaction. We found that the system organizes itself into a self-similar, time-invariant structure characterized by a scaling striation-thickness distribution (STD) which becomes asymptotically independent of the initial conditions. In this paper, we use a similar algorithm to simulate systems with finite rates of reaction; we explore the effects of the initial conditions mimicking imperfect mixing, the rate of reaction, and the reaction order on the evolution of the system. For simplicity, we uncouple the fluid mechanics from diffusion and reaction: the only role assigned to the fluid mechanics is to generate the initial lamellar structure. However, as has been noted in the past, fluid mechanical stretching can also be incorporated into the model simply by introducing a transformation of the time scale.[1–3]

The problem is quite rich and several types of evolution are possible, depending on the relative rates of stretching, diffusion, and reaction. The simplest situation occurs when the rate of diffusional mixing is much larger than the *intrinsic* rate of reaction; in such a case, the system becomes homogeneous before much reaction occurs, and the *overall* rate of reaction is determined only by chemical kinetics. [It is important to distinguish between the intrinsic (local) and the overall (global) rates of reaction: while the intrinsic rate of reaction is determined

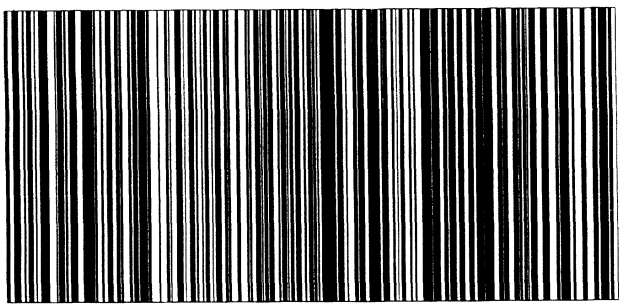

FIG. 1. Initial condition of an idealized one-dimensional lamellar system with distributed thicknesses; the thicknesses obey a prescribed distribution, but their sequence is random. Black and white regions represent alternate lamellae of A and B.

only by chemical kinetics, the overall rate of reaction depends also on the spatial distribution of reactants.] However, in cases where the rate of reaction is similar to or larger than the rate of diffusion, it is necessary to simultaneously account for mixing and reaction.

Systems involving diffusion and reaction have attracted considerable attention in recent years within the physics community.[7-12] Most studies to date can be grouped into two categories: (i) simulations of particles undergoing a given type of motion and reaction, and (ii) theoretical studies in terms of correlation functions in Fourier space. However, from the point of view of investigating the effects of mixing, both approaches are somewhat impractical: in the first approach it is impossible to consider enough particles to be able to characterize in detail effects such as the initial spatial distribution of reactants, whereas in the second approach information is lost when the system is represented in Fourier space. The lamellar model is able to overcome most of these difficulties; since this method is based on a direct simulation of the concentration field, it retains a full description of the state of the system at all times.

A detailed description of the method can be found in a previous publication.[6] At $t=0$, two reactants A and B are placed in alternate lamellae (Fig. 1). The lamellae have thicknesses distributed according to a prescribed STD $f(s,0)$, which gives the frequency of occurrence of lamellae of thickness s at time $t=0$. The reactants interdiffuse and undergo a reaction $A+B\rightarrow 2P$, where P is an inert product. The diffusion coefficient D is the same for all species, $D=1$ in units of length squared divided by unit time.

The evolution of such a system is given by the diffusion-reaction equation

$$\frac{\partial c_i}{\partial t}=D\frac{\partial^2 c_i}{\partial z^2}+r, \quad i=A,B \ , \tag{1}$$

where c_i is the concentration of either A or B at a given position and time, z is the spatial coordinate in the direction transverse to the interfaces of the lamellae, and r is the local rate of reaction. In this paper, we consider rates of reaction of the form

$$r=-k_r(c_A c_B)^{\alpha} \ , \tag{2}$$

where k_r is the reaction constant and α ranges from 0.5 to 3. The initial conditions for A and B lamellae are, respectively,

$$c_A(z,0)=C_{A0}, \quad c_B(z,0)=0 \ , \tag{3a}$$

$$c_A(z,0)=0, \quad c_B(z,0)=C_{B0} \ , \tag{3b}$$

and for simplicity we use periodic boundary conditions. Most of the work in this paper considers bimolecular kinetics, that is, $\alpha=1$.

Equation (1) can be expressed in terms of the dimensionless variables $\tau=t/T$, $\zeta=z/L$, and $y_i=c_i/C_0$, where T, L, and C_0 are time, length, and concentration scales as yet undefined. Substitution of Eqs. (2) for $\alpha=1$ into Eq. (1) and transformation of variables yields

$$\frac{\partial y_A}{\partial \tau}=\left[\frac{DT}{L^2}\right]\frac{\partial^2 y_A}{\partial \zeta^2}+k_r C_0 T y_{Ay_B} \ , \tag{4a}$$

$$\frac{\partial y_B}{\partial \tau}=\left[\frac{DT}{L^2}\right]\frac{\partial^2 y_B}{\partial \zeta^2}+k_r C_0 T y_{Ay_B} \ , \tag{4b}$$

where the dimensionless quantities DT/L^2 and $k_r C_0 T$ can be used to define the diffusional time scale $T_D=L^2/D$ and the reaction time scale $T_R=1/k_r C_0$. The evolution of the system is determined by the values of T_D and T_R: systems with the same $f(s,0)$ and the same second Damköhler number, $\mathcal{D}_{II}=T_D/T_R=k_r C_0 L^2/D$, evolve in identical manner.[13]

Because of the initial segregation of A and B, the product of $c_A(z,0)$ and $c_B(z,0)$ is zero everywhere and very little reaction occurs for short times. The initial evolution of the concentration field is governed by diffusion, and during this stage the overall rate of reaction is controlled by the chemical kinetics. If $\mathcal{D}_{II}\approx 0$, the system becomes homogeneous before significant reaction occurs, and the chemical kinetics control the overall rate of reaction for all later times. On the other hand, if $\mathcal{D}_{II}\rightarrow\infty$, A and B react as soon as they meet, and diffusion controls the overall rate of reaction for all times. However, for the wide intermediate case, a characterization of the system based on the initial conditions might be misleading (see also Table 9.1 in Ref. 1.) As time increases, variations of concentration over small length scales are erased by diffusion, and the characteristic length scale of the concentration field increases with time. Simultaneously, the average concentration of reactants $C[=\int c(z,t)dz/\int c(x,0)dz]$ decreases due to the reaction (the conversion X is defined as $1-C$). As a result of the diffusion-reaction process, both DT/L^2 and $k_r C_0 T$ decrease with time, and it is uncertain whether diffusion or chemical kinetics determines the evolution of the system for long times.

INFINITE RATES OF REACTION: SELF-ORGANIZING SCALING BEHAVIOR

In a system where $k_r=\infty$, species react as soon as they meet, and the reaction occurs only at *reaction planes* (interfaces between regions of different reactants). The overall rate of reaction is given by the product of the number of reaction planes and the average magnitude of the concentration gradient of the reactants at the reaction planes. The distribution in striation thickness adds complexity to the problem: subparts of the system are stoichiometrically imbalanced, and the planes move. The motion of the planes causes the spatial structure to evolve in time; thin lamellae are consumed by thicker neighbors, which merge into even thicker lamellae.

The spatial distribution of reactants determines the overall rate of reaction, which obeys two different kinetic regimes for short and long times.[6]

(i) For short times, most lamellae are much larger than the diffusional length scale $\delta(t)=(Dt)^{1/2}$, and the concentration gradients at both sides of each reaction plane are the same as if the lamellae were semi-infinite. The overall rate of reaction is given by

$$\frac{dC}{dt} = -k_1 C(0) N(t) t^{-1/2} , \tag{5a}$$

where $k_1 \approx 9 \times 10^{-4}$ is a "short-time kinetic coefficient," obtained from numerical results, and which is independent of the initial conditions. The number of reaction planes, which is equal to the number of surviving lamellae $N(t)$, is given by

$$\ln[N(t)] = \ln[N(0)] - \frac{2}{N(0)} \int_0^{s_i(t)} f(s,0) ds , \tag{5b}$$

where $s_i = (t/0.2747)^{1/2}$. The constant 0.2747 is the root of the transcendental equation $\text{erf}[s_i/(4t)^{1/2}] = \frac{1}{2}$ (see Ref. 6).

(ii) For long times, the system has only one independent length scale, $\delta(t) = (Dt)^{1/2}$, and its structure is characterized by scaling behavior. The STD evolves into a self-similar, scale-invariant form that is independent of the initial conditions. In this regime, the average concentration gradient at the reaction planes is approximately given by $C(t)/S(t)$, where $S(t)$ is the mean striation thickness, and the rate of reaction is given by

$$\frac{dC(t)}{dt} \approx -\frac{N(t)C(t)}{S(t)} \approx -k_2 C(t) N(t)^2 , \tag{6a}$$

where $k_2 \approx 7 \times 10^{-6}$ is a "long-time kinetic coefficient," also a numerical result, and $N(t)$ is given by

$$N(t) \approx k_3 t^{-1/2} , \tag{6b}$$

where $k_3 \approx 0.216$ is another numerically determined coefficient.[6] Substitution of Eq. (6b) into Eq. (6a) produces

$$\frac{dC(t)}{dt} \approx -C(t)^{(1+k_4)/k_4} , \tag{7}$$

a fractal kinetic expression, where $k_4 = k_2 k_3^2$ [i.e., $C(t)$ decays as $t^{-\gamma}$, where γ is a "critical" exponent].

In many applications, the rate of reaction is of the same or smaller magnitude than the rate of diffusional mixing, and the occurrence of a scaling regime is in question. The main objective of this paper is to determine whether or not scaling survives for $k_r < \infty$. We seek to establish the necessary conditions for the occurrence of scaling and to quantify the effects of the kinetic parameters α and k_r [see Eq. (2)] on the evolution of the system. In the final section, we develop a model that predicts the overall rate of reaction for all times.

THE SIMULATION ALGORITHM

The system is simulated by a large array of nodal points, divided into pieces corresponding to alternating A lamellae and B lamellae. The thicknesses of these lamellae obey the initial STD $f(s,0)$; however, since the lamellae are placed in random order, the thicknesses of neighbors are uncorrelated. At time $t = 0$, nodes in A lamellae are assigned $c_A = 1$, $c_B = 0$, and nodes in B lamellae are assigned $c_A = 0$, $c_B = 1$. The initial concentration scale C_0 is therefore $C_0 = C_{A0} = C_{B0} = 1$, making $c_A = y_A$ and $c_B = y_B$; since c_A and c_B are dimensionless and initially unity, we drop C_0 from all subsequent expressions. The initial amounts of A and B are identical, and due to the stoichiometry of the reaction, they remain identical for all times; nonstoichiometric cases are left for future work.

By contrast with the infinite rate of reaction case, the STD becomes meaningless once the diffusion-reaction process starts. As time increases, the reactants interdiffuse, the striations become blurred, and it becomes necessary to characterize the structure of the system in a different way. At any given time, the system is completely described by the concentration profiles $c_A(z,t)$ and $c_B(z,t)$; let us consider one of them, i.e., $c_A(z,t)$. The profile has a set of local maxima at locations $z_M(t)$ and a set of local minima at locations $z_m(t)$. We use $z_M(t)$ and $z_m(t)$ to divide the array into portions denoted *domains*, bounded by subsequent maxima and minima of $c_A(z,t)$. For $t \approx 0$, $z_M(0)$ and $z_m(0)$ are at the centers of the lamellae, and the domains can be constructed from the striations by adding the contiguous halves of each pair of neighboring striations.[2] The thicknesses of the domains, which are the distances between subsequent maxima and minima of $c_A(z,t)$, are denoted the *domain widths* w. The values of w are distributed, and we denote this *domain-width distribution* (DWD) as $h(w,t)$. Note the difference between striation thicknesses (distances at $t = 0$ between locations where $c_A = c_B = 0$) and domain widths [distances at any time between minima and maxima of $c_A(z,t)$]. In the same way as the STD was used to characterize the structure of systems with infinite rate of reaction,[6] we use the DWD to characterize the evolving structure of systems where the rate of reaction is finite. The mean value of w,

$$W(t) = \left[\int_0^\infty w h(w,t) dw \right] \Big/ \left[\int_0^\infty h(w,t) dw \right] , \tag{8}$$

is denoted the *mean domain width* and is used as one of the characteristic length scales in the system; the other characteristic length scale is the diffusional length scale $\delta(t) = (Dt)^{1/2}$. In order to be able to compare simulations involving different initial STD's, we define the initial length scale $L = S(0) = W(0) = 1$ unit length, therefore making $T_D = L^2/D = 1$.

To achieve enough accuracy at the small length scales initially present in the system, we need to use a large number of nodal points and a very small time step. Because of this, the common numerical approaches would require large amounts of CPU time. Following our previous work for the infinite rate of reaction case,[6] we use an algorithm based on the fractional-step method,[14] which solves the diffusion-reaction equation using a two-step procedure; the first step considers only diffusion and the second considers only reaction.

In order to complete the simulations within reasonable computer time, we continuously monitor $W(t)$. Each time $W(t)$ doubles its initial value $W(0)$, we divide the system into pairs of nodes, and substitute each pair of nodes by a single node, which is assigned values of c_A, c_B, and c_P that are the average of the pair; this operation is called a *contraction*. Since each contraction reduces the thicknesses of all diffusional domains by half, in order to preserve a consistent time scale, we multiply Δt by four. These contractions allow the system to achieve conver-

sions of 95% and times $t \approx 100$ after about 10^5 iterations. After vectorizing and optimizing of the code, each simulation is completed in about five hours of CPU time in a Convex C210. The entire set of calculations reported in this paper was completed in less than 500 hours of CPU time.

We check the algorithm in two ways: first, we run simulations for increasingly large values of k_r; as k_r increases, the results from these simulations asymptotically verify previous results for infinite rate of reaction, a case for which the split time-step algorithm has been thoroughly checked.[6] Second, we simulate the system using a different method where the entire right-hand side of Eq. (1) is evaluated at once using a fourth-order Runge-Kutta algorithm (RKA). The results produced by the RKA are nearly identical to those obtained using the fractional-step method; the relative errors in the average concentration obtained by the different methods are smaller than 1×10^{-4} for all times. However, although the same contractions were implemented in both methods, simulations using the RKA usually required about 40 times more CPU time than those using the fractional-step method. The algorithm reported here enabled us to efficiently simulate a very large system undergoing diffusion and reaction, making it possible to consider a distribution of length scales in the imperfectly mixed initial state.

THE SIMULATIONS

The results in this paper correspond to three types of simulations. In the first group of simulations we consider systems composed of 1200 lamellae, undergoing a reaction with bimolecular kinetics. We use three different initial conditions: (i) a linearly decreasing initial STD $f(s,0)=a-bs$, (ii) a random initial STD in which all thicknesses between five and 500 nodes occur with the same frequency, and (iii) a normal (Gaussian) initial STD with standard deviation of 125 nodes. In order to improve the accuracy of the results, we run several simulations for each set of parameters: for the linear case, we run ten simulations for each value of $k_r=1$, 10, 100, and 1000; for the random and normal cases, we run ten simulations for $k_r=10$ and one for $k_r=1,100,1000$. Different simulations corresponding to each initial STD and each value of k_r have the same list of thicknesses ordered in a different random sequence.[6] We measure the average concentration C, the total number of domains N, the mean domain width W, and the DWD as a function of time. Results presented in this paper are the average for all the simulations corresponding to each initial STD and each value of k_r.

The second type of simulation concentrates on the dynamics of reaction at short times and small length scales. We study the evolution of a single lamella of one of the reactants (i.e., A) surrounded by much larger regions of the other reactant. The local rate of the reaction is again $r=-k_r c_A c_B$, and we run simulations for $k_r=0.3-3000$ and for initial thickness $L=15-960$ nodes. We follow the evolution of the concentration profiles $c_i(z,t)$, and also measure the overall rate of reaction as a function of time for each value of k_r and L. In order to compare the effects of different initial thicknesses for the lamella, for these simulations we define 1 unit length as equal to 30 nodes.

In the third type of simulation, we consider the effects of the reaction order on the evolution of the system: for $k_r=100$, we explore values of α in the range 0.5–3.0. Because of the stiffness introduced by $\alpha\neq1$, we integrate the reaction step in the split time-step algorithm by means of a RKA. In this case we consider systems composed of only 200 lamellae (these simulations consume a considerable amount of CPU time—20 to 100 hours each—and the results are based on one simulation for each value of α). For $\alpha<1.0$, stiffness is a serious problem; we deal with it by using an inverse transformation $\chi_i(z,t)=1/c_i(z,t)$ and solving the reaction step in terms of $\chi_i(z,t)$.

SCALING BEHAVIOR: EVOLUTION OF THE DWD

At $t=0$, the structure of the system is characterized by the initial DWD, $h(w,0)$. Since a domain of width w is composed of two half-lamellae whose combined initial thicknesses add up to $2w$, the initial frequency of domains with width w is given by $\frac{1}{2}\int_0^{2w} f(s,0)f(2w-s,0)ds$. The normalized $h(w,0)$ is then related to the initial STD by

$$h(w,0)=\frac{\frac{1}{2}\left[\int_0^{2w} f(s,0)f(2w-s,0)ds\right]}{\left[\int_0^{\infty} dw\int_0^{2w} f(s,0)f(2w-s,0)ds\right]} . \quad (9)$$

However, as time increases, the spatial structure of the system evolves, and the DWD changes: small domains disappear; large domains grow and merge into even larger domains. As the diffusion-reaction process goes on, the frequency of small domains decreases, the DWD develops a tail in the large w region, the number of surviving domains decreases, and $W(t)$ increases.

This complicated evolution shows the symptoms of self-organization: the long-time DWD's in Figs. 2(a) (linear initial STD), 2(b) (random initial STD), and 2(c) (normal initial STD) all look very similar (all three figures correspond to $k_r=10$). Systems having different initial DWD's seem to evolve into a universal distribution of domain widths that is independent of the initial conditions. Following our previous development for infinite rate of reaction,[6] we assume a universal, time-invariant scaling solution for the DWD at moderate to large conversions, and test this hypothesis using scaling techniques.[15–17] We postulate that

$$w^2 h(w,t)=g(w/W(t)) , \quad (10)$$

where $g(y)$ is the scaling solution and $y=w/W(t)$ is the scaling argument. This scaling technique requires that some moments of $h(w,t)$ converge.[8] (For further details, see the Appendix, which has been included for completeness.)

The scaling hypothesis is verified by results from the simulations: Fig. 3(a) shows that the curves in Fig. 2(a)

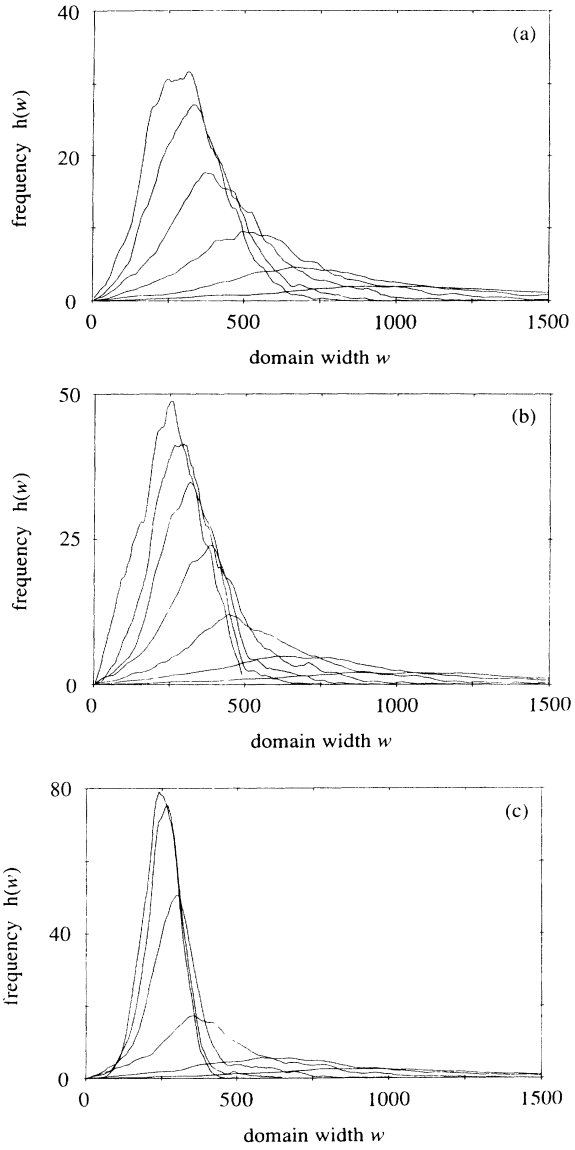

FIG. 2. (a) Evolution of the domain-width distribution (DWD) for a system with a linear initial striation-thickness distribution (STD). The system is initially composed of 1200 lamellae with thicknesses following a distribution $f(s,0)=a-bs$, with $a=3.2386$, $b=0.004\,266$. As time increases, the conversion increases and the DWD changes; the frequency for small values of w decreases, and a tail develops in the large w region. The DWD is shown for $X=0.093,0.201,0.33,0.52,0.645,0.745$; $t=0.06,0.121,0.241,0.483,0.966,1.931$; $k_r=10$. (b) Evolution of the DWD for a system with a random initial STD. The system is initially composed of 1200 lamellae whose thicknesses are randomly distributed; all thicknesses in the range 5–500 occur with the same probability. The DWD evolves very similarly to the previous case. The figure shows the DWD for $X=0.101,0.22,0.36,0.55,0.688,0.78,0.834$; $t=0.06,0.121,0.241,0.483,0.965,1.931,3.862$; $k_r=10$. (c) Evolution of the DWD for a system with a normal initial STD. The system is initially composed of 1200 lamellae with thicknesses in the range of 5–500 nodes and a standard deviation of 125 nodes, and evolves in a similar fashion as in the previous two cases. The figure shows the DWD for $X=0.22,0.38,0.58,0.74,0.83,0.88$; $t=0.1,0.2,0.4,0.8,1.62,3.25$; $k_r=10$.

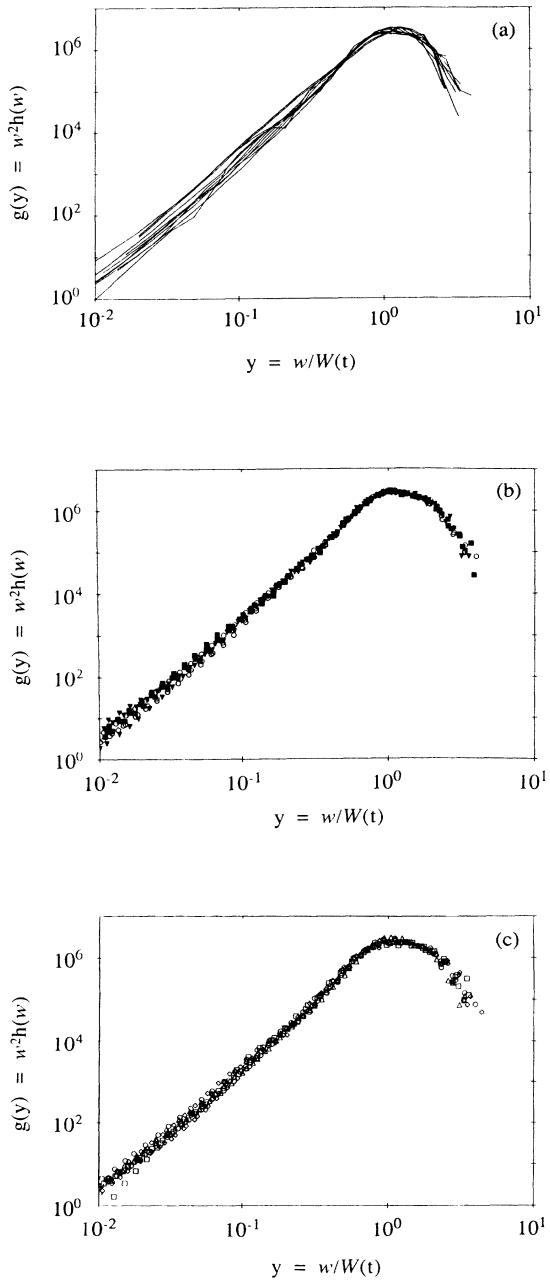

FIG. 3. (a) Scaling behavior present in the evolution of the DWD. The distributions in Fig. 2(a) are plotted as $g(y)=w^2h(w,t)$ vs $y=w/W(t)$, where $W(t)$ is the mean domain width at time t; as X increases, the curves asymptotically collapse into a master curve. The results correspond to an initially linear STD and are the average of ten simulations; the initial condition is shown as a double line. (b) Comparison of the scaled DWD's for systems with linear (circles), random (triangles), and normal (squares) initial STD's. In each case, three curves are shown, all of them for $X\geq 0.5$. The curves are nearly identical, demonstrating that the scaled DWD $g(y)=w^2h(w,t)$ is independent of the initial conditions. (c) The scaled DWD for a system with a linear initial STD, $X\geq 0.5$; $k_r=1,10,100,1000$. The curves are shown for each value of k_r, all of them for $X\geq 0.5$. The curves overlap, demonstrating that the scaling DWD $g(y)=w^2h(w,t)$ is independent of the value of k_r.

overlap when plotted in rescaled form. As time increases, the curves asymptotically enter a master curve, and the scaled DWD becomes time invariant. All DWD's corresponding to $X \geq 0.4$ are indistinguishable from one another; the divergences between them are due to the limited size of the system.

The universality of the scaling solution with respect to the initial conditions is demonstrated in Fig. 3(b), where long-time DWD's corresponding to different initial STD's overlap when plotted in scaled form. This scaling behavior seems to be independent of the value of k_r as well; the same type of data collapse is observed for any fixed value of k_r in the range $k_r = 1-1000$. As Fig. 3(c) shows, long-time DWD's corresponding to *different values of* k_r overlap when plotted in scaled form.

The universality in the long-time dynamics of the system can also be observed in Fig. 4(a), which shows the evolution of the number of surviving domains $N(t)$ for different initial STD's. Similarly to the infinite rate of reaction case,[6] for long times $N(t)$ becomes independent of the initial conditions. Figure 4(b) shows that, for long enough times, $N(t)$ has a very weak dependence on k_r: increasing k_r at any fixed time by a factor of 1000 decreases $N(t)$ by a factor of 2. In all cases, for long times $N(t)$ decays as $N(t) \approx t^{-1/2}$ (as was the case for $k_r = \infty$), and therefore the main domain width $W(t) \approx 1/N(t)$ increases with time as $W(t) \approx t^{1/2}$. This is particularly important because it clearly shows that for long times the system has only one independent length scale, the diffusional length scale $\delta(t) \approx (Dt)^{1/2}$, and $W(t)$ differs from $\delta(t)$ only by a multiplicative constant.

For long enough times, as diffusion takes control of the dynamics and $\delta(t)$ becomes the only independent length scale, the evolution of the system becomes asymptotically identical to that of a system where $k_r = \infty$. The evolution of the average concentration of reactants, which is the focus of the next section, also demonstrates that diffusion is the dominant process for long times.

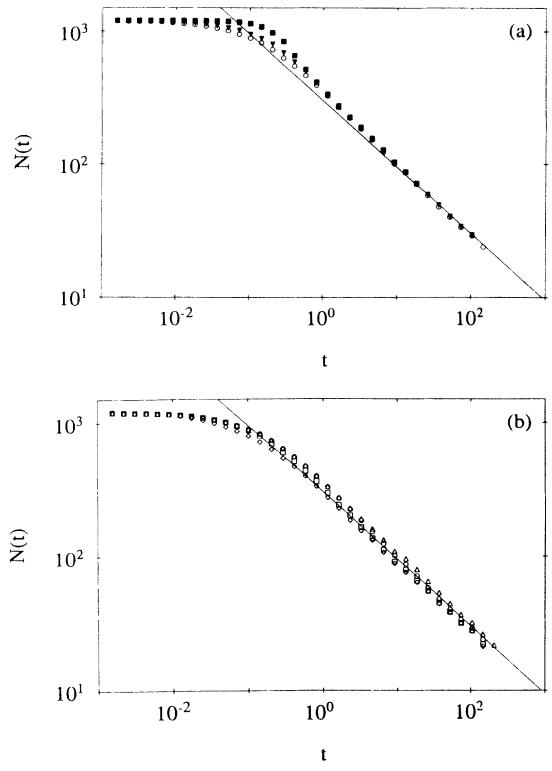

FIG. 4. (a) $N(t)$, the number of surviving domains, decays as $N(t) \approx t^{-1/2}$ for long times. The results correspond to systems with linear (circles), random (triangles), and normal (squares) initial STD's, $k_r = 10$. A curve corresponding to $N(t) = 300t^{-1/2}$ is also included for comparison. The values of $N(t)$ for all initial STD's seem to enter the same curve at long times. (b) The long-time decay of $N(t)$ for a system with a linear initial STD, $k_r = 1$ (triangles), 10 (circles), 100 (squares), and 1000 (diamonds). The value of $N(t)$ has a weak dependency with k_r; increasing k_r 1000 times decreases $N(t)$ by a factor of 2. In all cases, $N(t)$ decays as $t^{-1/2}$ for long times; a curve corresponding to $N(t) = 300t^{-1/2}$ is included for comparison.

EVOLUTION OF THE AVERAGE CONCENTRATION OF REACTANTS

Figure 5 shows the evolution of $C(t)$ for systems with linear initial STD, bimolecular kinetics, $k_r = 1$, 10, 100, 1000, and ∞. As k_r decreases, the decay of $C(t)$ is delayed; however, as time increases, the value of $C(t)$ corresponding to a particular value of k_r eventually becomes identical to the value of $C(t)$ corresponding to $k_r = \infty$. For times $t \geq 20/k_r$, the offset between the values of $C(t)$ corresponding to a particular k_r and to $k_r = \infty$ is less than 0.05. The same behavior is observed for systems with random and normal initial STD's. In all cases, a simulation with an infinite rate of reaction (by far the best known case and the easiest and least expensive to simulate) gives an excellent prediction for $C(t)$ for $t \geq 20/k_r$.

The interpretation of these observations is straightforward: for bimolecular kinetics and long times, the intrinsic rate of reaction eventually becomes much larger than the rate of diffusion; reaction zones are depleted, and the reactants segregate again. Subsequently, diffusion and reaction occur in series, and the overall rate is determined by the slower process, which in this case is molecular

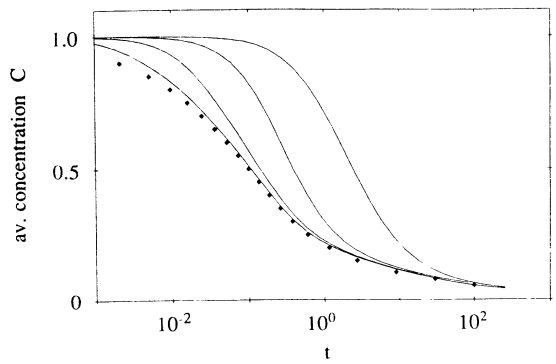

FIG. 5. Evolution of the average concentration of reactants $C(t)$. The curves correspond to a system with a linear initial STD, $k_r = 1, 10, 100, 1000$; the diamonds correspond to $k_r = \infty$. As k_r decreases, the decay of $C(t)$ is delayed. For long enough times $t \geq 20/k_r$, the values of $C(t)$ corresponding to a finite value of k_r and to $k_r = \infty$ become identical.

diffusion. Since diffusion controls the dynamics of the system for long times, the evolution of the system becomes asymptotically identical to that of a system with an infinite intrinsic rate of reaction, which is characterized by scaling behavior. For bimolecular kinetics, the effect of k_r is largely to determine *when* this "diffusional takeover" occurs, not *whether* it occurs or not.

For times $t > W(0)^2/4D$, the diffusional length scale $\delta(t)$ overrides $W(0)$ (the characteristic length introduced by the initial conditions), and $\delta(t)$ becomes the only characteristic length in the system; we observe $\delta(t) \approx W(t) \approx t^{1/2}$. It should be noticed that en route to scaling, the system undergoes two independent transitions: (i) from a system that is controlled by the intrinsic chemical kinetics to a system that is controlled by diffusion, and (ii) from a system with several characteristic lengths to a system with only one characteristic length $\delta(t)$. These transitions might occur in any order, depending on the value of $\mathcal{D}_{II}$.

It should be noted that this "diffusional takeover" shows some dependency on the reaction order. Figure 6 shows results corresponding to the second type of simulation, which considers systems where $r = -k_r(c_A c_B)^\alpha$, $k_r = 100$. The curves correspond to 200 lamellae, linear initial STD, α in the range 0.5–3.0; results corresponding to infinite intrinsic speed of reaction are also shown for comparison. The effect of increasing the reaction order is somewhat similar to the effect of decreasing the reaction constant: the higher the order, the longer it takes $C(t)$ to decay to a given value. Different behaviors are observed depending on the value of α (i) For $\alpha < 1.5$, for long enough times the values of $C(t)$ corresponding to finite and infinite rates of reaction become identical. (ii) For $1.5 < \alpha < 2.5$, the values of $C(t)$ for finite k_r and for $k_r = \infty$ do not become identical in the explored range $X(t) < 0.95$; however, $C(t)$ decays with a power law of time that has the same exponent for both finite and infinite k_r. (iii) For $\alpha > 2.5$, the decay of $C(t)$ still follows a power-law relationship, but the exponent is equal to $1/(1-2\alpha)$, characteristic of the chemical kinetics. This is consistent with previous calculations[6,18] which indicate that, for $k_r = \infty$, $C(t)$ decays as $C(t) \approx t^{-1/4}$. Since the slowest decay law should prevail, the condition for a kinetically controlled regime becomes $1/(1-2\alpha) > -\frac{1}{4}$, or $\alpha > 2.5$.

It is apparent that the system can experience at least two types of evolution, depending on the reaction order. (i) For $\alpha < 1.5$, the rate of diffusion decays faster than the local rate of reaction. Nonuniformities in the concentration field persist for all times, and eventually determine the evolution of the system. For long times, diffusion takes control of the dynamics of reaction, the intrinsic chemical kinetics become irrelevant, and the behavior of the system becomes identical to that of a system where $k_r = \infty$. (ii) For $\alpha > 2.5$, the intrinsic rate of reaction decays faster than the rate of diffusion; the diffusionally controlled regime is never achieved, and after a period diffusional mixing in which the nonuniformities of the concentration field are erased, the decay of $C(t)$ is controlled by the chemical kinetics. The situation is less clear in the interval $1.5 < \alpha < 2.5$: $C(t)$ decays with the power law corresponding to the scaling regime, but it does not become identical to the values of $C(t)$ corresponding to $k_r = \infty$. Our results are not conclusive enough to make a stronger statement for this range of values of α; more extensive simulations considering larger systems appear to be necessary in order to obtain better bounds for the behavior of the system and to improve the characterization of the different regimes.

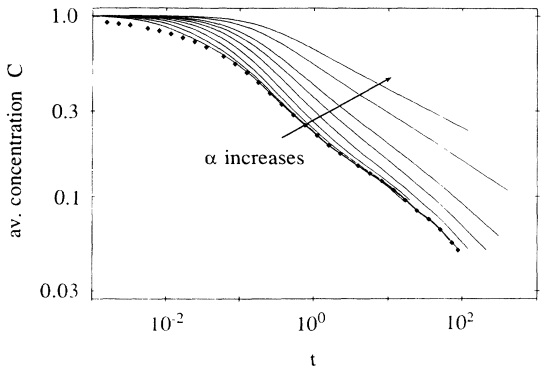

FIG. 6. $C(t)$ for systems with the local rate of reaction $r = -k_r(c_A c_B)^\alpha$, $k_r = 100$. The curves correspond to 200 lamellae, $\alpha = 0.5$, 0.75, 1.0, 1.25, 1.5, 1.75, 2, 2.5, and 3.0. Results corresponding to $k_r = \infty$ are also shown (diamonds). As α increases, the decay of $C(t)$ is delayed; however, for $\alpha < 1.5$, all curves become asymptotically identical to the values corresponding to $k_r = \infty$ for long enough times. For $1.5 < \alpha < 2.5$, the curves for finite rates of reaction do not seem to verify the values for infinite rate of reaction, but $C(t)$ decays with the same power law that is characteristic of the scaling regime. For $\alpha > 2.5$, the decay of $C(t)$ is still expressed by a power-law relationship, but the exponent is $1/(1-2\alpha)$, characteristic of the chemical kinetics.

It is important to note that, since for $\alpha < 1.5$ we observe that for long times the system evolves similarly to a system where $k_r = \infty$; in particular, since $C(t) \approx t^{-1/4}$ and $N(t) \approx 1/W(t) \approx t^{-1/2}$, the amount of unreacted materials in each domain, $C(t)/N(t) \approx t^{1/2}$, *increases* with time, i.e., the system *unmixes*. A similar result was observed before for infinitely fast reactions between particles;[18] these results contradict what is often assumed in the chemistry and chemical engineering literature, namely, that for reactions of finite speed, after an initial mixing period, the system achieves homogeneity and from then on the chemical kinetics dominate the evolution of the system.

In what follows, we concern ourselves with the first case, $\alpha < 1.5$, which seems to be the most realistic and applicable; in particular, we focus on $\alpha = 1$. For this case, the system becomes diffusionally controlled for long times, scaling behavior describes the evolution of the spatial structure, and $C(t)$ becomes identical to the value of $C(t)$ corresponding to $k_r = \infty$. The kinetic regimes described by Eqs. (5)–(7) can be used to predict the overall rate of reaction for long times; and our problem is therefore reduced to finding a model able to describe the evolution of the system for short times. In order to accomplish this, we need to study in more detail the dynamics of an isolated lamella surrounded by much larger neighbors. These dynamics can be used to predict the short-

time behavior of the entire array of 1200 lamellae. This is the focus of the next two sections.

REACTION DYNAMICS OF A SINGLE LAMELLA WITH INFINITE NEIGHBORS

In this section, we consider the dynamics of reaction of a single lamella with initial thickness in the range $L=17-960$ nodes, undergoing a bimolecular reaction with dimensionless reaction constant k_r in the range $k_r=0.3-3000$. Since concentration gradients vanish at $z=\pm\infty$, the total rate of reaction is given by

$$L\frac{\partial C}{\partial t}=-k_r\Phi(t)\ , \tag{11}$$

where $\Phi(t)$ is the reaction integral

$$\Phi(t)=2\int_0^\infty c_A c_B dz\ , \tag{12}$$

and $z=0$ corresponds to the center of the finite lamella.

Figure 7 shows the evolution of $\Phi(t)$ for different values of k_r. For short times, little reaction occurs; however, as the reactants interdiffuse, the reaction zones build up, and $\Phi(t)$ increases as $t^{1/2}$. However, since the rate of diffusion monotonically decreases, $\Phi(t)$ eventually reaches a maximum value, and subsequently it decreases. The evolution of $\Phi(t)$ depends on the value of k_r. (i) For large k_r, the reaction is fast compared to diffusion, and the reaction zones begin to be depleted before the concentration gradients reach the center of the finite lamella. The maximum of $\Phi(t)$ occurs at $t_M\approx 1/k_r \ll L^2/4D$; under these conditions, the reactants remain mostly segregated, and the overall rate of reaction is controlled by the rate at which diffusion can transport materials into the reaction zone. In the interval $t_M<t<L^2/4D$, this rate of transport decays with time as if the lamellae at both sides of each reaction zone were infinite, and during this period

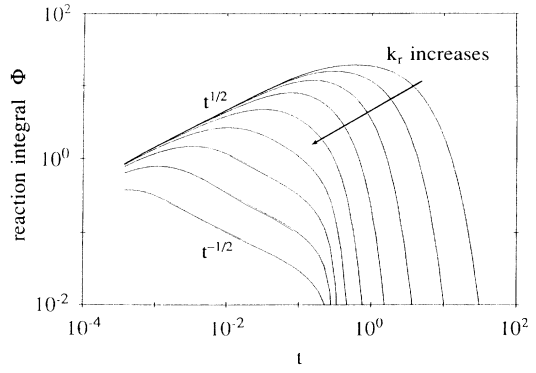

FIG. 7. Evolution of $\Phi(t)$ $(=2\int_0^\infty c_A c_B dz)$ for different values of k_r, ranging from $k_r=0.3$ at the top, to $k_r=3000$ at the bottom, for a single lamella with much larger neighbors. For short times, $\Phi(t)$ increases as $t^{1/2}$, goes through a maximum, and then decreases monotonically. For large k_r, the maximum of each curve occurs at $t\approx 1/k_r$; subsequently, $\Phi(t)$ decays as $t^{-1/2}$ until $t\approx L^2/4D$, and after that, $\Phi(t)$ decays exponentially.

we observe that $\Phi(t)\approx t^{-1/2}$. At $t\approx L^2/4D$, the concentration gradients reach the center of the finite lamella; and after that $\Phi(t)$ decays exponentially. (ii) For small values of k_r the concentration gradients reach the center of the finite lamella before $\Phi(t)$ begins to decay. The dynamics are much more complex: diffusional mixing and reaction occur simultaneously, and the role of the different parameters is less clear. However, for this case $\Phi(t)$ also goes through a maximum, and then decays at an exponential rate.

The results shown in Fig. 7 also represent $\Phi(t)$ for lamellae of different initial thicknesses. The evolution of the concentration field depends on three parameters: ζ, τ, and $\mathcal{D}_{\rm II}$ $(=k_r C_0 L^2/D)$, and the reaction integral is given by

$$\Phi(t)=2\int_0^\infty c_A(\zeta,\tau,\mathcal{D}_{\rm II})c_B(\zeta,\tau,\mathcal{D}_{\rm II})dz \tag{13}$$

$$=2L\int_0^\infty c_A(\zeta,\tau,\mathcal{D}_{\rm II})c_B(\zeta,\tau,\mathcal{D}_{\rm II})d\zeta$$

$$=2LF(t/T_D,\mathcal{D}_{\rm II})\ , \tag{14}$$

where F is a function of t/T_D and $\mathcal{D}_{\rm II}$ only. Equation (14) can be used to transform the set of curves in Fig. 7, which has k_r as a parameter, into a new set that has L as a parameter. Increasing L has similar effects on the evolution of $\Phi(t)$ as increasing k_r. (i) For large values of L, $\Phi(t)$ reaches its maximum value before the concentration gradients reach the center of the lamella. There is a period in which the reaction zones evolve as if both lamellae at each side of each reaction zone were infinite, and the overall rate of reaction is controlled by the rate at which diffusion can transport reactants into the reaction zones. (ii) For smaller values of L, the concentration gradients reach the center of the finite lamella before $\Phi(t)$ achieves its maximum value; the reaction zones spread throughout the finite lamella, and the evolution of $\Phi(t)$ is complicated. In order to be able to predict the evolution of $\Phi(t)$ for either small k_r or small L, we need to know the evolution of $c_A(z,t)$ and $c_B(z,t)$ for those conditions.

For diminishing values of k_r, the evolution of $c_i(\zeta,\tau,\mathcal{D}_{\rm II})$ must approach the limiting behavior corresponding to $k_r=0$; in the limit $\mathcal{D}_{\rm II}\to\infty$ (no reaction) the evolution of $c_i(\zeta,\tau,\mathcal{D}_{\rm II})$ is purely diffusive. For an A lamella surrounded by infinite B lamellae, $k_r=0$, we have

$$c_A(\zeta,\tau,0)=\tfrac{1}{2}\{\mathrm{erf}[(\tfrac{1}{2}-\zeta)/(4\tau)^{1/2}] + \mathrm{erf}[(\tfrac{1}{2}+\zeta)/(4\tau)^{1/2}]\}\ , \tag{15a}$$

$$c_B(\zeta,\tau,0)=1-\tfrac{1}{2}\{\mathrm{erf}[(\tfrac{1}{2}-\zeta)/(4\tau)^{1/2}] + \mathrm{erf}[(\tfrac{1}{2}+\zeta)/(4\tau)^{1/2}]\}\ . \tag{15b}$$

The simulations indicate that, for small k_r, the evolution of $c_A(\zeta,\tau,\mathcal{D}_{\rm II})$ is very closely approximated by

$$c_A\approx\tfrac{1}{2}C_A(\tau,\mathcal{D}_{\rm II})\{\mathrm{erf}[(\tfrac{1}{2}-\zeta)/(4\tau)^{1/2}] + \mathrm{erf}[(\tfrac{1}{2}+\zeta)/(4\tau)^{1/2}]\}\ , \tag{16a}$$

$$c_B \approx 1-[1-C_A(\tau,\mathcal{D}_{II})/2] \times\{\mathrm{erf}[(\tfrac{1}{2}-\zeta)/(4\tau)^{1/2}]+\mathrm{erf}[(\tfrac{1}{2}+\zeta)/(4\tau)^{1/2}]\} . \quad (16b)$$

The shape of the profile c_A corresponding to $k_r=0$ is preserved for small, nonzero values of k_r; the only difference between Eqs. (15a) and (16a) is the prefactor $C_A(\tau,\mathcal{D}_{II})$, which is the average concentration of A at time τ. A small rate of reaction changes the total amount of reactant present at a given time, but not the way in which this reactant is distributed in space.

Equations (16a) and (16b) are further simplified by recalling that, for large enough τ

$$\mathrm{erf}[(\tfrac{1}{2}-\zeta)/(4\tau)^{1/2}]+\mathrm{erf}[(\tfrac{1}{2}+\zeta)/(4\tau)^{1/2}] \approx(\pi\tau)^{-1/2}\exp(-\zeta^2/4\tau) , \quad (17)$$

thus obtaining

$$c_A(\zeta,\tau,T_r/T_D)\approx[(4\pi\tau)^{-1/2}C_A(\tau,T_r/T_D)] \times\exp(-\zeta^2/4\tau) , \quad (18a)$$

$$c_B(\zeta,\tau,T_r/T_D)\approx 1-[2-C_A(\tau,T_r/T_D)] \times(4\pi\tau)^{-1/2}\exp(-\zeta^2/4\tau) . \quad (18b)$$

As is shown in Fig. 8, the agreement between the observed profile $c_A(\zeta,\tau,\mathcal{D}_{II})$ and the prediction of Eq. (18a) is extremely good. Similar agreement is obtained for $c_B(\zeta,\tau,\mathcal{D}_{II})$ (not shown in the figure). Equations (18a) and (18b) can now be used to estimate $\Phi(t)$; substitution of Eqs. (18a) and (18b) into Eq. (13) and straightforward integration produce

$$\Phi(\tau,\mathcal{D}_{II})\approx LC_A(\tau,\mathcal{D}_{II})\{1-(8\pi\tau)^{-1/2}[2-C_A(\tau,\mathcal{D}_{II})]\} \quad (19)$$

and Eq. (19), together with Eq. (11), allow us to predict $\Phi(\tau,\mathcal{D}_{II})$ for small values of k_r, $\tau\geq 1/8\pi$. For $\tau<1/8\pi$, $\Phi(t)$ is given, to a very good approximation, by the following interpolation between the $\Phi(t)\approx t^{1/2}$ and the $\Phi(t)\approx t^{-1/2}$ regimes:

$$\Phi(t)\approx L(8\tau/\pi)^{1/2}/(1+2k_r\tau^2)^{1/2} . \quad (20)$$

In Fig. 9, we compare the prediction of Eqs. (11), (19), and (20) (curves) with results from the simulations (dots). The "jump" in the curves corresponds to the transition between Eq. (20) (short times) and Eq. (19) (long times) which occurs at $\tau\approx 1/(8\pi)$. It is apparent that for thin lamellae (or for small k_r) this prediction works very well for all times. For thick lamellae, Eqs. (11) and (20) still give a very good prediction of the evolution of $\Phi(t)$ for small τ, but the method fails for large τ. However, since our objective here is to obtain a model for short times (long-time behavior is predicted by the scaling regime) this failure is of little consequence.

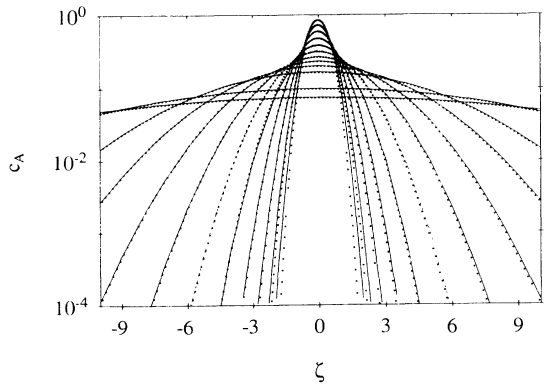

FIG. 8. Evolution of the concentration profile $c_A(z,t)$ for an A lamella, $L=30$ nodes, surrounded by much larger regions of B. The curves correspond to $k_r=0.3$, $t=1,2,3,5,10,30,50,100,200,300,500,1000$. The concentration profile $c_A(z,t)$ is very nearly Gaussian; the observed profile (dots) is accurately predicted by $c_A(z,t)\approx[(4\pi\tau)^{-1/2}C_A(\tau)]\exp(-\zeta^2/4\tau)$ (continuous curves), where $\zeta=z/L$ and $z=0$ corresponds to the center of the A lamella.

A SIMPLIFIED MODEL FOR SHORT TIMES

A combination of the results from the preceding section allows the prediction of the overall rate of reaction for the whole 1200-lamellae system. Consider a reaction zone developing between lamellae of initial thicknesses s_i and s_j, $s_i<s_j$. The initial rate of reaction is zero; however, as time increases, the reactants interdiffuse and a reaction zone builds up in the region between the lamellae. Concentration gradients develop at the reaction zones and penetrate the lamellae; the depth of this penetration is proportional to the diffusional length scale, $\delta(t)\approx(Dt)^{1/2}$. Locations inside the lamellae that are farther away than $\delta(t)$ from the center of the reaction zone remain unaffected by the diffusion-reaction process. For short enough times $0<t<s_i^2/4D$, $\delta(t)$ is smaller than $s_i/2$, and the actual values of s_i and s_j do not affect the

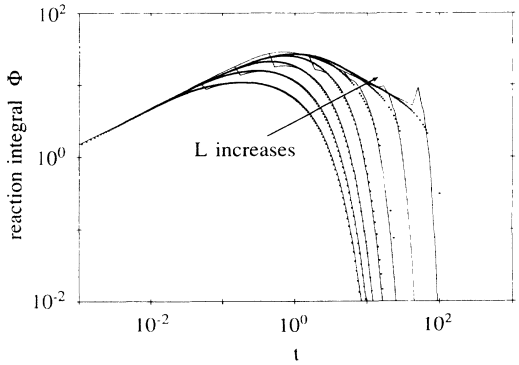

FIG. 9. Evolution of $\Phi(t)$ for $L=17$, 30, 53, 96, 170, 300, and 530 nodes, for a single lamella with much larger neighbors; comparison of the prediction of Eqs. (11), (19), and (20) (curves) with results from the simulations (dots).

evolution of the reaction zone; Eqs. (11) and (20) alone will give an excellent prediction of the reaction integral for this interval. However, this prediction fails as soon as the gradients reach the center of the smaller lamella in the pair, well before the reaction is completed. We use instead Eqs. (11), (19), and (20) to obtain an approximate prediction of $\Phi(\tau)$ in the more extended interval $0<t<s_j^2/4D$; on average, this prediction is accurate until the gradients reach the center of the larger lamella in the pair, and if $s_i \ll s_j$, the reaction zone extinguishes before the prediction fails. Equations (11), (19), and (20) give a complete prediction of the evolution of the reaction integral for such a reaction zone; in this interval, the rate of reaction depends only on the value of s_i.

The short-time model is based on a statistical description of the system, which is regarded to be composed of 1200 reaction zones, each of them developing between two lamellae of thicknesses s_i and s_j. We characterize each reaction zone only by the smaller of both thicknesses, s_i. In order to compute the overall rate of conversion for the entire system $\Phi'(t)$, we calculate $\Phi(t)$ for each value of s_i, multiply it by the number of pairs of lamellae where the smaller thickness is s_i, and integrate for all values of s_i. The frequency $r(s_i)$ of pairs of lamellae where the smaller thickness is s_i can be obtained from $f(s,0)$:

$$r(s_i)=2f(s_i,0)\left[\int_{s_i}^{\infty} f(s,0)ds\right]\Big/\left[\int_0^{\infty} f(s,0)ds\right] . \quad (21)$$

The rest of the model is straightforward: we solve Eqs. (11), (19), and (20) for 100 evenly spaced values of s_i covering the range of $f(s,0)$. The values of $\Phi(s_i,t)$ are added as

$$\Phi'(t)=\sum_{s_i} r(s_i)\Phi(s_i,t)\Delta s , \quad (22)$$

where $\Phi'(t)$ is the estimated value of the reaction integral for the whole system and Δs is the spacing between values of s_i. For a widely distributed, randomly ordered STD, the probability that the lamellae at each side of a reaction zone have similar thicknesses is small, and in this case the model works best.

For long times, reaction zones interact and eventually merge; at some time $t \approx W(0)^2/4D$, Eqs. (11), (19), (20) fail to predict $\Phi(t)$ for many surviving reaction zones, and the short-time model breaks down. However, for large enough values of k_r, the system becomes diffusionally controlled before the short-time model fails. The overall rate of reaction for the diffusion-controlled regime is given by Eqs. (5)–(7), and a combination of the different predictions gives us the complete evolution of the overall rate of reaction. To estimate the overall rate of reaction, we use Eq. (22) for conversions $X(t)\leq 0.35$, an average of Eqs. (7) and (22) for $X(t)$ between 0.35 and 0.5, and Eq. (7) for $X(t)>0.5$. Figure 10(a) compares this prediction with results from simulations for a system with linear initial STD; $k_r=1,10,100,1000$. While for $k_r \geq 100$ the prediction is very good for all times, for $k_r \leq 10$ the prediction remains good for short times, but becomes poor for long times. This occurs because the

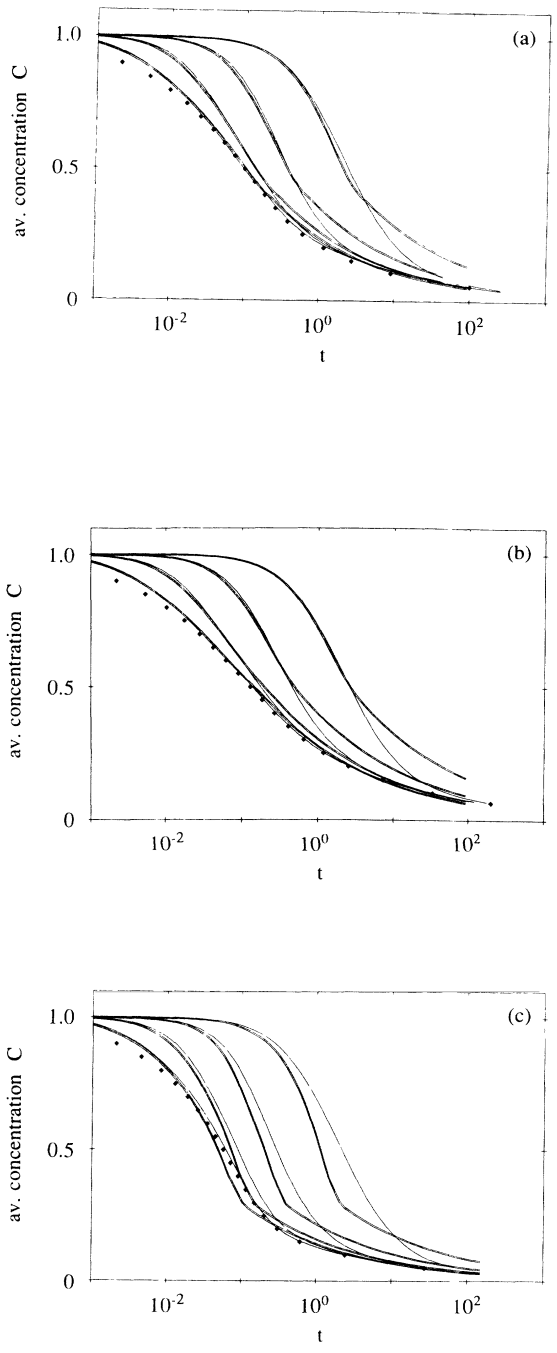

FIG. 10. (a) The observed $C(t)$ (single curves) and the prediction of the model (double curves) for a linear initial STD, $k_r=1,10,100,1000$; values for $k_r=\infty$ (diamonds) are also included. For $k_r \geq 100$, the prediction of the model is very good for all times. For $k_r \leq 10$, the prediction of the model remains good for short times, but becomes poorer for long times. (b) Observed $C(t)$ and the prediction of the model for a random initial STD, $k_r=1,10,100,1000$; values for $k_r=\infty$ are also shown [symbols as in (a)]. The performance of the model for this case is similar to the previous one. (c) Observed $C(t)$ and the prediction of the model for a normal initial STD, $k_r=1,10,100,1000$; values for $k_r=\infty$ are also shown [symbols as in (a)]. The magnitude of the errors is considerably larger than those corresponding to the other two initial STD's.

short-time model fails before the system becomes diffusionally controlled. However, for long times, we can predict $C(t)$ using an alternative procedure: $C(t)$ becomes asymptotically identical to the value of $C(t)$ corresponding to a system where $k_r=\infty$, which is efficiently predicted by Eqs. (5)–(7).

The performance of the model depends to some extent on the initial STD; the amount of error is similar for linear [Fig. 10(a)] and random [Fig. 10(b)] initial STD's, but is much larger for normal initial STD [Fig. 10(c)]. The normal STD has less dispersion than the random and linear STD's; the fraction of reaction zones bounded by lamellae of similar thicknesses is larger, and Eqs. (11), (19), and (20) fail at an earlier time. However, in this case also the system becomes diffusionally controlled for long times, and the results for $k_r=\infty$ give a good prediction of $C(t)$ for all values of k_r.

CONCLUSIONS

We have shown that a lamellar system with distributed striation thickness can be efficiently simulated using a numerical procedure that uncouples diffusion and reaction, computing their effects in a sequential manner. The efficiency of the numerics depends on the type of reaction considered, but even strongly nonlinear cases can be simulated using this approach at the expense of a larger, but still reasonable, amount of CPU time.

Scaling techniques reveal that the system undergoes critical self-organization; a universal, time-invariant distribution of length scales emerges as the conversion increases. Two transitions occur in the system, producing this critical behavior: (i) the system becomes diffusionally controlled, and (ii) the diffusional length scale becomes the only characteristic length. Scaling is observed for a wide class of chemical reactions and is considerably independent of the chemical kinetics, which becomes irrelevant in the diffusion-controlled regime.

As diffusion takes control of the dynamics, the decay of reactants becomes much slower than predicted by the chemical kinetics. In practical terms, this slowdown implies that larger reactors and longer residence times are required to achieve a given conversion. Since the diffusional time scale increases with the square of the characteristic length scale, the initial degree of fluid-mechanical mixing, measured as the initial value of the mean striation thickness $S(0)$, has very strong effects on the evolution of the system.

The importance of self-organized criticality is apparent throughout this work. This approach to reaction dynamics is relatively unexploited and it is likely that several other interactions between reaction dynamics, mixing processes, and critical self-organization remain to be discovered. Many specific issues related to effects of stoichiometric imbalances, continuous fluid-mechanical stretching, multiple reactions leading to selectivity effects, and mixing of more than two reactive materials, remain to be explored.

ACKNOWLEDGMENTS

This work is pertinent to projects supported by the U.S. Department of Energy, Office of Basic Energy Sciences, and the U.S. Air Force Office of Scientific Research. The use of the Convex C210 was supported by the Materials Research Laboratory of the University of Massachusetts. We are grateful to Professor Robert Guyer, Physics Department, University of Massachusetts, for many enlightening discussions.

APPENDIX

Consider a distribution $f(s,t)$ where f is the frequency of occurrence of a given value of s at time t. This distribution can be represented as a family of curves f versus s that have t as a parameter; examples of such a distribution are given in Figs. 2(a)–(c). The distribution is said to have scaling properties, or to be self-similar in time, if a simple stretching (shape-preserving) transformation of variables

$$f \rightarrow g = K(t) f \ , \tag{A1}$$

$$s \rightarrow y = s/\sigma(t) \tag{A2}$$

makes the curves overlap, or, in other words, if

$$g(y) = K(t) f(s,t) \tag{A3}$$

is time independent. For this transformation to be useful, we need to be able to determine $K(t)$ and $\sigma(t)$ *a priori*. Let us consider the first moment of such a scaling distribution,

$$m_1(t) = \int_0^\infty s f(s,t) ds \ , \tag{A4}$$

and assume that $m_1(t)$ converges. Replacing (A2) and (A3) into (A4), we obtain

$$m_1(t) = [\sigma(t)^2/K(t)] \int_0^\infty y g(y) dy \ . \tag{A5}$$

Since $\int_0^\infty y g(y)$ is equal to a constant C_1,

$$K(t) = C_1 \sigma(t)^2 / m_1(t) \ , \tag{A6}$$

and

$$g(y) = C_1 \sigma(t)^2 f(s,t) / m_1(t) \ . \tag{A7}$$

In order to determine $\sigma(t)$, let us consider the ratio of any two successive (convergent) moments of $f(s,t)$

$$m_i/m_{i-1} = \frac{\left[\int_0^\infty s^i f(s,t) ds\right]}{\left[\int_0^\infty s^{i-1} f(s,t) ds\right]} \tag{A8}$$

$$= \frac{\sigma(t)^{i-1}\left[\int_0^\infty y^i g(y) dy\right]}{\sigma(t)^{i-2}\left[\int_0^\infty y^{i-1} g(y) dy\right]} \tag{A9}$$

$$= \frac{\sigma(t)\left[\int_0^\infty y^i g(y) dy\right]}{\left[\int_0^\infty y^{i-1} g(y) dy\right]} \ ; \tag{A10}$$

since the terms in large parentheses are constants, we conclude that $\sigma(t)$ can (at least in principle) be estimated

up to a constant as the ratio of any pair of successive moments of $f(s,t)$. Replacing Eq. (A2) into (A7) and further rearranging produces

$$y^2 g(y) = g'(y) = C_1 s^2 f(s,t)/m_1(t) . \quad \text{(A11)}$$

For systems that conserve "mass" (or, in other words, that have a constant first moment), Eq. (A11) is further simplified to

$$g'(y) = C_2 s^2 f(s,t) , \quad \text{(A12)}$$

where $C_2 = C_1/m_1(t)$. This is the scaling transformation used in this paper.

[1]See Chap. 9 in J. M. Ottino, *The Kinematics of Mixing: Stretching, Chaos, and Transport* (Cambridge University Press, Cambridge, England, 1989).

[2]J. M. Ottino, J. Fluid Mech. **114**, 83 (1982).

[3]W. E. Ranz, in *Mixing of Liquids by Mechanical Agitation,* edited by J. J. Ulbrecht and G. K. Patterson (Gordon and Breach, New York, 1977).

[4]D. B. Spalding, in *Proceedings of the 17th Symposium (International) on Combustion, Pittsburgh, 1978* (The Combustion Institute, Pittsburgh, 1978), pp. 431–439.

[5]F. J. Muzzio and J. M. Ottino, Phys. Rev. Lett. **63**, 47 (1989).

[6]F. J. Muzzio and J. M. Ottino, Phys. Rev. A **40**, 7182 (1989).

[7]K. Kang and S. Redner, Phys. Rev. A **32**, 435 (1985).

[8]P. G. J. Van Dongen and M. H. Ernst, J. Stat. Phys. **50**, 295 (1988).

[9]G. H. Weiss, R. Kopelman, and S. Havlin, Phys. Rev. A **39**, 466 (1989).

[10]H. Schnorer, V. Kuzovkov, and A. Blumen, Phys. Rev. Lett. **63**, 805 (1989).

[11]F. J. Muzzio and J. M. Ottino, Phys. Rev. A **38**, 2516 (1988).

[12]B. J. West, R. Kopelman, and K. Lindenberg, J. Stat. Phys. **54**, 1429 (1989).

[13]R. Chella and J. M. Ottino, Chem. Eng. Sci. **39**, 551 (1984).

[14]E. S. Oran and J. P. Boris, *Numerical Simulation of Reactive Flows* (Elsevier, New York, 1987).

[15]P. C. Hohenberg and B. I. Halperin, Rev. Mod. Phys. **49**, 435 (1977).

[16]D. Stauffer, Phys. Rep. **54**, 1 (1979).

[17]P. Meakin, in *Phase Transitions and Critical Phenomena,* edited by C. Domb and J. L. Lebowitz (Academic, New York, 1988), Vol. 12, and references therein.

[18]D. Toussaint and F. Wilczek, J. Chem. Phys. **78**, 2642 (1983).